Laser and Particle Beams (2007), *25*, 465–469. Printed in the USA.
 0263-0346/07 $20.00
DOI: 10.1017/S0263034607000572

Spectrally resolved X-ray scatter from laser-shock-driven plasmas

D. RILEY,[1] F.Y. KHATTAK,[1] E. GARCIA SAIZ,[1] G. GREGORI,[2,3] S. BANDYOPADHYAY,[2] M. NOTLEY,[2] D. NEELY,[2] D. CHAMBERS,[4] A. MOORE,[4] AND A. COMLEY[4]

[1]School of Mathematics and Physics, Queen's University Belfast, Belfast, United Kingdom
[2]CCLRC Rutherford Appleton Laboratory, Oxon, United Kingdom
[3]Clarendon Laboratory, University of Oxford, Oxford, United Kingdom
[4]AWE plc, Reading, Berks, United Kingdom

(RECEIVED 23 February 2007; ACCEPTED 22 May 2007)

Abstract

We report spectrally resolved X-ray scattering data from shock compressed foils illustrating the feasibility of X-ray Thomson scattering experiment on a sub-kilo joule laser system. Sandwich targets consisting of CH/Al/CH were shock compressed using ~1 ns laser pulses. Separate 270 ps laser pulses were used to generate an intense source of Ti-He-α ($1s^2$-$1s2p^1P$) radiation which was used as a probing source of 4.75 keV photons. The spectrum of scattered photons was recorded at a scattering angle of 82° with a CCD fitted spectrometer using a PET crystal in von-Hamos geometry. Although spectral resolution was used to separate the scatter from any background, the resolution was limited by source broadening. The relative level of scatter at different times in the sample history was measured by varying the delay between the shock driving beams and the back-lighter beams. We have compared the scatter spectra with simulations based on two different models of the L-shell bound-free contribution.

Keywords: Plasma; Shock; X-ray Scatter

1. INTRODUCTION

In recent years, spectrally resolved X-ray scattering has been developed, mainly on multi-kJ laser systems, for probing dense plasmas (Glenzer *et al.*, 2003; Landen *et al.*, 2001; Gregori *et al.*, 2003, 2004; Tsytovich, 1996; Redmer *et al.*, 2005; Schollmeier *et al.*, 2006, Peng *et al.*, 2005). This has been motivated by the desire to reproduce the significant success of Thomson scattering in the optical regime for lower density plasmas and to extend it to the difficult to diagnose, warm dense matter (WDM) regime (Ng *et al.*, 2005; Lee *et al.*, 2002). So far this technique has been successful in diagnosing electron temperature in radioactively heated plasmas (Glenzer *et al.*, 2003) and by comparing the contributions of strongly and weakly bound and free electrons, a technique for determining the average ionization of a sample has been developed (Gregori *et al.*, 2004, 2006). These experiments have generally been carried out with back-scattering in the regime where the Thomson scattering parameter, α, is generally <1. Physically, this means that the scattering spectrum reflects short spatial scale thermal motion of the electrons rather than the longer scale collective motions that are probed when $\alpha > 1$. In fact, attaining $\alpha > 1$ is not trivial, due to the degeneracy effect on collective motions and the requirements on probe collimation, bandwidth and coherence (Gregori *et al.*, 2006) and the definition of α has to be modified (Landen *et al.*, 2001). The experiment presented here was the first attempt at the VULCAN laser facility (Danson *et al.*, 2005) to carry out spectrally resolved X-ray Thomson scatter. It was the first attempt to carry out such an experiment with double sided shock compression as a method of generating the sample.

2. EXPERIMENT

In a recent experiment using the VULCAN laser system at the Rutherford Appleton Laboratory, we have attempted to probe a laser-shock compressed sample in the forward direction, where we expect $\alpha \sim 1$. The experiment is shown schematically in Figure 1. Two 70 J beams of 0.53 μm laser light of ~1 ns duration were focused onto a sample foil at 45° to

Address correspondence and reprint requests to: D. Riley, School of Mathematics and Physics, Queen's University Belfast, University Road, BT7 1NN, UK. E-mail: d.riley@qub.ac.uk

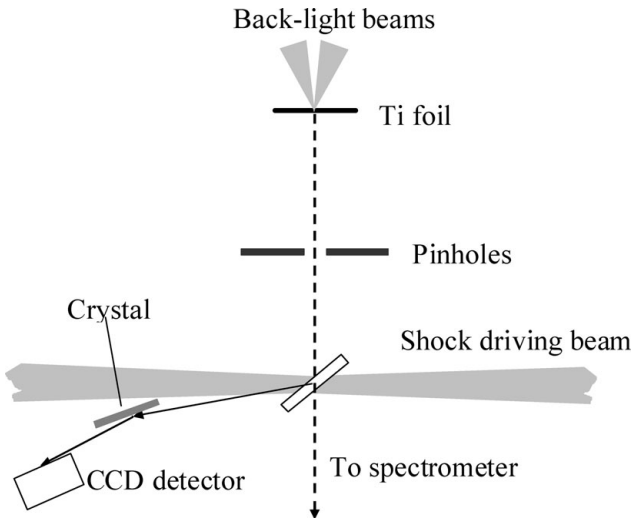

Fig. 1. Schematic of the experimental setup. The distances are not to scale. For clarity, the extensive screening of the CCD from the back-lighter is not shown.

both beams which typically consisted of a CH/Al/CH sandwich with thicknesses 4.5/6/4.5 μm. The foils were 5 mm × 5 mm in lateral dimension. With phased zone plates the focal spot, projected onto the target, was 1.5 mm × 2.3 mm and flat topped. The beams had a sharp rise over 250 ps to a peak intensity of 7×10^{12} Wcm^{-2} followed by a slow fall to zero over 900 ps. These are the shock driving beams for producing the "sample."

Two shorter (∼270 ps full-width at half maximum, FWHM) 100 J pulses, synchronized to the longer pulses to an accuracy of ∼30 ps, were focused onto a 3 μm thick Ti foil at $\sim 2 \times 10^{15}$ Wcm^{-2} to create a bright source of Ti-He-alpha radiation at 4.75 keV. The conversion efficiency to He-alpha was estimated using a flat crystal spectrometer fitted with a Si (111) crystal at $\sim 2 \times 10^{12}$ photons/J. The photons from this source passed through a system of two pinholes and fell onto the target in a cone of ∼7° divergence. When projected onto the target at 45°, this cone illuminated an ellipse of 1 × 1.4 mm and contained $\sim 5 \times 10^{12}$ photons on target. Most of the X-ray beam then passed through the sample target to a "back-lighter monitor" spectrometer which was a CCD fitted with a flat quartz (10–12) crystal.

The alignment of sample target, pinholes, and back-lighter target, all mounted through Martock stages on a single target-stage with kinematic base, was achieved by measuring their position to an accuracy of about 20 μm with respect to the base using an external alignment rig. This rig was fitted with high magnification telescopes coupled to CCDs viewing the targets from three different directions. The sample target, pinhole system, and the backlighter target could be individually moved and adjusted relative to each other using the Martock micro-positioning stages. An exact replica of the target-stage with a single wire and a cross-wire target at the defined position of the backlighter target and sample target, respectively, was used to align the backlighter beams and heating beams onto the targets inside the chamber, using obscuration. When the actual target-stage was substituted, we could be sure that the system was aligned such that X-rays from the back-lighter were centered on the shocked region. Previous experience with such a system on femto-second scale laser experiments, where the target foils remained after the shot, gives us confidence that the alignment of the centers of the probing X-rays and shock driven region was better than 50 μm.

The Ti-He-alpha photons scattered at 82° were collected with a PET crystal in von-Hamos geometry. Several calibration spectra were taken, by placing a Ti foil at the sample foil position and heating it with one of the shock driving beams with the phase plate removed. This allowed a calibration for the wavelength scale and was carried out both prior to and after scatter shots and the position of the peaks was reproducible to about 0.5 mÅ accuracy. While this geometry does not fully satisfy the source coherence requirements (effectively equivalent to having the scatter $\alpha > 1$) for observing collective modes (Gregori *et al.*, 2006), it establishes a working platform for future experiments aimed to directly explore plasma dynamics in warm dense matter using a sub-kJ laser facility.

The density and temperature history of the entire foil was calculated using the HYADES, radiation hydrodynamics code (Larsen & Lane, 1994) including multi-group radiation transfer and the SESAME equation of state (Lyon & Johnson, 1992). Results for one particular probing time are shown in Figure 2 as an example of the plasma conditions generated. For these conditions, we expect the Al foil to display strong coupling with a coupling parameter, $\Gamma = (Z^*e)^2/R_i k T_i > 50$; where R_i is the average ion separation, T_i is the ion temperature and Z* is the average ionization.

3. SCATTER DATA AND SIMULATIONS

Figure 3 shows typical scatter data at different back-lighter delays. A calibration shot is included for comparison in

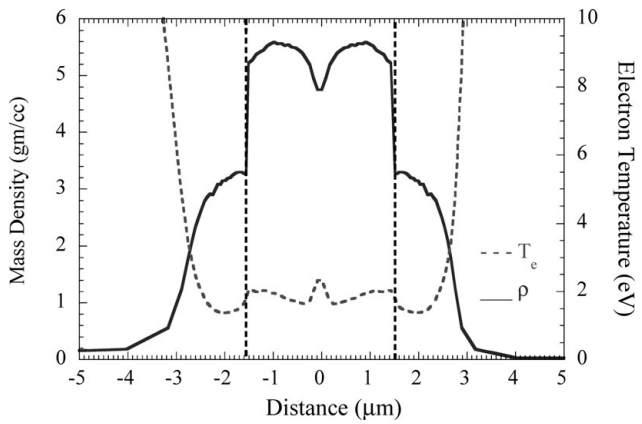

Fig. 2. Typical simulation conditions at a delay of 0.5 ns from the peak of the pulse, using the Hyades code. See text for more discussion. The vertical dashed lines mark the CH/Al boundaries.

https://doi.org/10.1017/S0263034607000572 Published online by Cambridge University Press

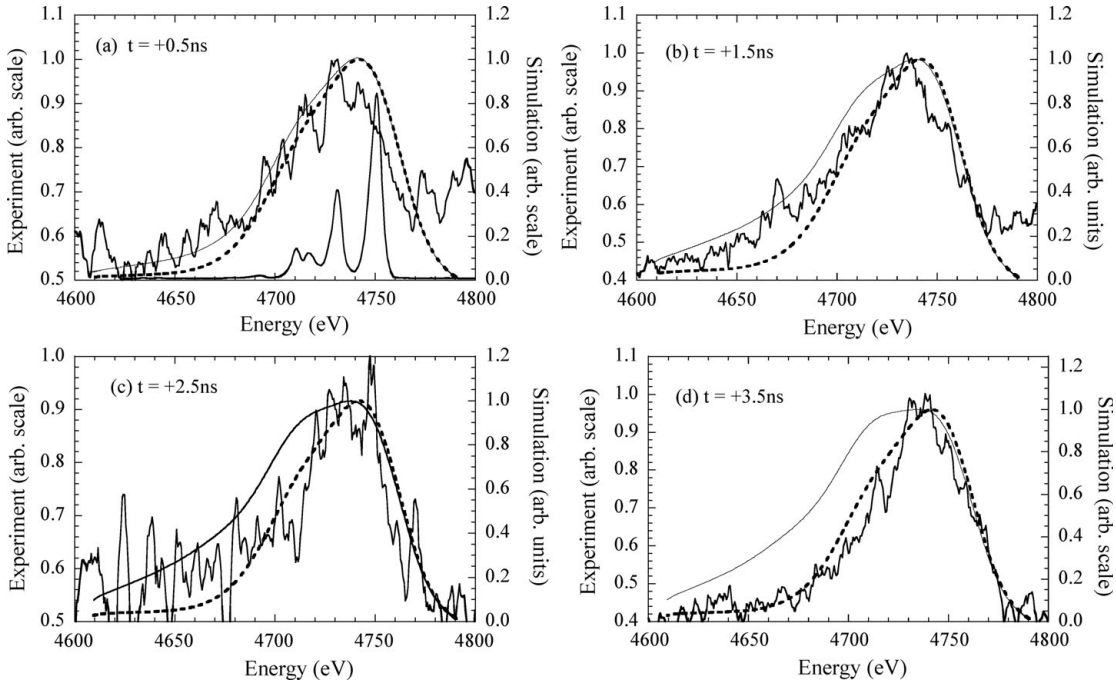

Fig. 3. Typical data at a delay of 0.5 ns to 3.5 ns from the peak of the pulse compared to simulation with source spectrum and broadening folded in. In the source spectrum is shown for comparison. For the simulations, the solid line uses the impulse approximation (Holm & Ribberfors, 1989) whilst the dashed line uses the Schumacher *et al.* (1974) profiles.

Figure 3a. We can see that the scatter data is not only broader but seems to have a peak shifted by a few mÅ from the wavelength of the principal $1s^2$-$1s2p^1P$ line at 2.6097Å. Simulations of the data are also shown and were carried out along lines similar to Gregori *et al.* (2003, 2004). In the absence of absolute calibration, both data and simulation are normalized to have a peak of unity and the data plot is corrected to account for the background level from the sample plasma. The basic terms for the simulation are described in Chihara (2000) and are shown in Eq. (1) below:

$$S(\omega, q) = |f(q) + \rho\,(q)|^2 S_{ii}(q, \omega) + Z_f S_{ee}(q, \omega) + Z_B \int S_{ce}(q, \omega - \omega') S_s(q, \omega')\, d\omega'. \quad (1)$$

The three terms on the right-hand side are, respectively, the coherent scatter from bound and free electrons, the incoherent free electron scatter and incoherent scatter arising from bound-free transitions. The scatter from the bound electrons is coherent despite the general incoherent nature of the source because the wavelength is of the order or larger than the ion radius and so, in a semi-classical picture, coherent oscillation of the electrons and subsequent re-radiation of the incoming photons occurs which is essentially elastic. Correlation between the ions as described by $S_{ii}(q,\omega)$ leads to angular structure. The code takes the density and temperature of the Al and uses the Thomas-Fermi (TF) model to derive the ionic form factor and average ionization. The free electron density and temperature are used in the random phase approximation (RPA) model to give the free electron scatter. An analytical fit to the OCP model is used to generate the static ion structure factor at the angle of scatter (Bretonnet & Derouiche, 1988). This fit gives a good approximation to the one component plasma (OCP) data of Galam and Hansen (1976) for the very high coupling parameters ($\Gamma > 50$) found in our case. The ion-electron structure factor is found using the Boercker and More (1986) formalism which is valid for high ion-ion coupling. Rather than use an average ion model of atomic structure for the bound-free contributions, we take the average Z* and make the very simple assumption that the plasma is made up from two ionization species, Z_{low} and $Z_{low} + 1$ in proportions such that the average ionization is Z* from the TF model. For lower ionization states we then use the accurate energy level data from a Hartree-Fock model and the Stewart-Pyatt continuum lowering model (Stewart & Pyatt, 1966) to find the binding energies of the *nl* levels. Two models of the Compton profiles for the bound-free incoherent scatter are used for comparison. First, we use equations from Holm and Ribberfors (1989) with first order corrections to the impulse approximation. This is not necessarily expected to be very accurate as the impulse approximation generally assumes that the ratio $E_B/E_C < 1$, where E_B is the binding energy of the electron in question and E_C is the usual Compton energy shift for a free electron at the same scatter angle. For our case ($E_C \sim 50$eV), this is not close to being true for the K-shell electrons and is marginal for L-shell electrons. The other form of Compton profiles is taken from Schumacher *et al.* (1975) which uses the form factor approximation but not the impulse approximation.

https://doi.org/10.1017/S0263034607000572 Published online by Cambridge University Press

In the simulations for Figure 3, we have folded in the Ti-He-alpha source spectrum, shown in Figure 3a, and added 36eV source broadening to account for the expected source size presented to the spectrometer. As we can see, the general shape is reproduced. The shift in the peak is a consequence of the asymmetric nature of the incident spectrum combined with the high level of broadening. We can see that using the Compton profiles described by Holm and Ribberfors leads to a reasonable fit to data at early time but we get a progressively worse fit at later times as it apparently overestimates the bound-free contribution from the L-shell electrons in the C and Al ions. Using the Schumacher profiles leads to a smaller contribution from bound-free incoherent scatter. The fit is acceptable at all times, but there is a noticeable underestimate of the scatter signal at photon shifts of $\sim$50–150 eV for all but the latest time. This suggests the bound free contribution is underestimated.

In Figure 4, we show the time history of total scatter for a short series of shots with different delays, compared to simulation. The error bars are based an estimate of the error in subtracting the background of signal due to continuum emission from the sample plasma; the reproducibility from shot to shot is seen at t = 2.5 ns, although based on two shots. The flat behavior at late time is not surprising since the number of atoms per unit area is roughly constant and plasma conditions vary slowly. Early in time, the rapid change in predicted coupling and hence ion-ion structure factor should lead to a rapid change in total cross-section, as seen by the simulation. Unfortunately, for operational reasons we were unable to complete a detailed time scan to resolve the peak at $\sim$1 ns delay. It is possible that, in a future experiment, with a long pulse back-lighter and a high sensitivity streak camera instead of a CCD, this behavior may be observed with high temporal resolution. The recent development of more sensitive streak cameras (Lerche *et al.*, 2004) may make this possible.

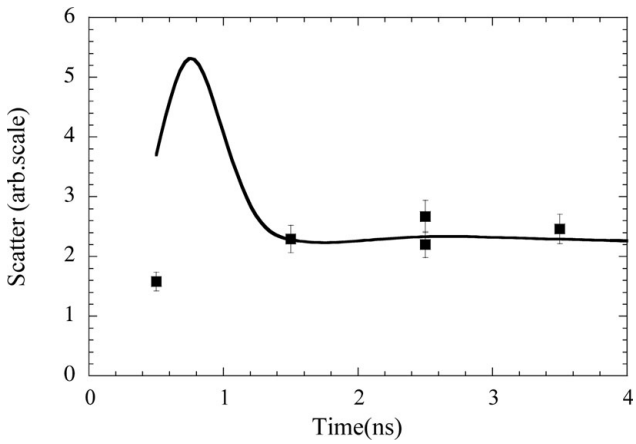

Fig. 4. Simulation of total scatter (solid line) calculated with bound-free Compton profiles from Schumacher et al. (see text) against time history of total scatter from a series of shots (squares). In the absence of absolute calibration the data and simulation have been scaled to agree at t = 2.5 ns where there are two consistent data shots.

4. SUMMARY

In summary, this work demonstrates the feasibility of performing X-ray Thomson scattering experiment on a moderate sized (sub-kJ) laser facility using crystal as a dispersive element. With two-dimensional focusing crystals it should be possible to get enough resolution and signal to noise ratio to better observe the L-shell bound-free contribution to the scattering. With better temporal resolution it should be possible to observe the temporal evolution of the coherent scatter as a function of time and relate this to the evolution of the ion-ion structure factor. This would be a valuable complementary measurement to the angularly resolved scatter at a fixed time (Riley *et al.*, 2000**).** During the preparation of this manuscript, a paper by Neumeyer *et al.* (2006) also, illustrating scatter from a sub-KJ system has been published.

ACKNOWLEDGEMENT

This work was supported by the UK Engineering and Physical Sciences Research Council under grant No. EP/C001869/1.

REFERENCES

Boercker, D.B. & More, R.M. (1986). Statistical-mechanics of a 2-temperature, classical plasma. *Phys Rev. A* **33**, 1859–1869.

Bretonnet, J.-L. & Derouiche, A. (1988). Analytic form for the one-component plasma structure factor. *Phys. Rev. B* **38**, 9255–9256.

Chihara, J. (2000). Interaction of photons with plasmas and liquid metals-photoabsorption and scattering. *J. Phys: Condens. Matter* **12**, 231–247.

Danson, C.N., Brummitt, P.A., Clarke, R.J., Collier, I., Fell, B., Frackiewicz, A.J., Hawkes, S., Hernandez-Gomez, C., Holligan, P., Hutchinson, M.H.R., Kidd, A., Lester, W.J., Musgrave, I.O., Neely, D., Neville, D.R., Norreys, P.A., Pepler, D.A., Reason, C., Shaikh, W., Winstone, T.B., Wyatt, R.W.W. & Wyborn, B.E. (2005). Vulcan petawatt: Design, operation and interactions at 5×10^{20} Wcm^{-2}. *Laser Part. Beams* **23**, 87–93.

Galam, S. & Hansen, J.-P. (1976). Statistical mechanics of dense ionized matter. VI. Electron screening corrections to the thermodynamic properties of the one-component plasma. *Phys. Rev. A* **14**, 816–832.

Glenzer, S.H., Gregori, G., Lee, R.W., Rogers, F.J., Pollaine, S.W. & Landen, O.L. (2003). Demonstration of spectrally resolved X-ray scattering in dense plasmas. *Phys. Rev. Lett.* **90**, 17500/1.

Gregori, G., Glenzer, S.H., Rozmus, W., Lee, R.W. & Landen, O.L. (2003). Theoretical model of X-ray scattering as a dense matter probe. *Phys. Rev. E* **67**, 026412.

Gregori, G., Glenzer, S.H., Rogers, F.J., Pollaine, P.W., Landen, O.L., Blancard, C., Faussurier, G., Renaudin, P., Khulbrodt, S. & Redmer, R. (2004). Electronic structure measurements of dense plasmas. *Phys. Plasmas* **11**, 2754–2762.

Gregori, G., Tommassini, R., Landen, O.L., Lee, R.W. & Glenzer, S.H. (2006). Limits on collective X-ray scattering imposed by coherence. *Europhys. Lett.* **74**, 637–643.

https://doi.org/10.1017/S0263034607000572 Published online by Cambridge University Press

Holm, P. & Ribberfors, R. (1989). 1st correction to the non-relativistic Compton cross-section in the impulse approximation. *Phys. Rev. A* **40**, 6251–6259.

Landen, O.L., Glenzer, S.H., Edwards, M.J., Lee, R.W., Collins, G.W., Cauble, R.C., Hsing, W.W. & Hammel, B.A. (2001). Dense matter characterization by X-ray Thomson scattering. *J. Quant. Spectrosc. Radiat. Transfer* **71**, 465–478.

Larsen, J.T. & Lane, S.M. (1994). Hyades–A plasma hydrodynamics code for dense plasma studies. *J. Quant. Spectrosc. Radiat. Transfer* **51**, 179–186.

Lee, R.W., Baldis, H.A,. Cauble, R.C., Landen, O.L., Wark, J.S., Ng, A., Rose, S.J., Lewis, C., Riley, D., Gauthier, J.C. & Audebert, P. (2002). Plasma-based studies with intense X-ray and particle beam sources. *Laser Part. Beams* **20**, 527–536.

Lerche, R.A., Mcdonald, J.W., Griffith, R.L., Vergel de Dios, G., Andrews, S., Huey, A.W. Bell, P.M., Landen, O.L., Jaanimagi, P.A. & Boni, R. (2004). Preliminary performance measurements for a streak camera with a large-format direct coupled charge-couple device readout. *Rev. Sci. Instrum.* **75**, 4042–4044.

Lyon, S.P. & Johnson, J.D. (1992). SESAME: The Los Alamos National Laboratory Equation of State Database LANL Group T-1 report LA-UR-92–3407.

Neumayer, P., Gregori, G., Ravasio, A., Koenig, M., Price, D., Widmann, K., Bastea, M., Landen, O.L. & Glenzer, S.H. (2006). Solid-density plasma characterization with x-ray scattering on the 200 J Janus laser. *Rev. Sci. Instrum.* **77**, 10F317.

Ng, A., Ao, T., Perrot, F., Dharma-Wardana, M.W.C. & Foord, M.E. (2005). Idealized slab plasma approach for the study of warm dense matter. *Laser Part. Beams* **23**, 527–537.

Peng, H.S., Zhang, W.Y., Zhang, X.M., Tang, Y.J., Zheng, W.G., Zheng, Z.J., Wei, X.F., Ding, Y.K., Gou, Y., Zhou, S.P. & Pei, W.B. (2005). Progress in ICF programs at CAEP. *Laser Part. Beams* **23**, 205–209.

Redmer, R., Reinholz, H., Ropke, G., Thiele, R. & Holl, A. (2005). Theory of X-ray Thomson scattering in dense plasmas. *IEEE Trans. Plasma Sci.* **33**, 77–84.

Riley, D., Woolsey, N.C., McSherry, D. & Nardi, E. (2000). X-ray scattering from a radiatively heated plasma. *J. Quant. Spectrosc. Radiat. Transfer* **65**, 463–470.

Schollmeier, M., Prieto, G.R., Rosmej, F.B., Schaumann, G., Blazevic, A., Rosmej, O.N. & Roth, M. (2006). Investigation of laser-produced chlorine plasma radiation for non-monochromatic X-ray scattering experiments. *Laser Part. Beams* **24**, 335–345.

Schumacher, M., Smend, F. & Borchert, I. (1975). Incoherent scattering of gamma rays by inner-shell electrons. *J. Phys. B: Atom. Molec. Phys.* **8**, 1428–1439.

Stewart, J.C. & Pyatt, K.D. (1966). Lowering of ionization potentials in plasmas. *Astrophys. J.* **144**, 1203.

Tsytovich, V.N. (1996). Collective quantum scattering in plasma. *Astropart. Physics* **5**, 285–298.

https://doi.org/10.1017/S0263034607000572 Published online by Cambridge University Press